10. J. White *et al.*, *Philos. Trans. R. Soc. London Ser. B* **314**, 1 (1986).
11. The *hlh-1* product in GLR cells was nuclear-localized and seen in embryos and larvae.
12. M. Thayer and H. Weintraub, *Cell* **63**, 23 (1990); R. A. Rupp and H. Weintraub, *ibid.* **65**, 927 (1991).
13. M. Edgley and D. Riddle, *Genet. Maps* **5**, 3.111 (1990); A. Coulson, J. Sulston, S. Brenner, J. Karn, *Proc. Natl. Acad. Sci. U.S.A.* **83**, 7821 (1986). Newer map data were from S. Kim (*lin-31*), R. Lee, R. Feinbaum, and V. Ambros (*lin-4* and *maDf4*), and M. Stern (*unc-85*).
14. R. E. Rosenbluth, C. Cuddeford, D. L. Baillie, *Genetics* **109**, 493 (1985).
15. The mutation *dpy-25*(*e817sd*), isolated by S. Brenner, causes animals to be shorter than normal (Dumpy). The severity of the mutation depends on dosage: homozygotes are extremely short while *dpy-25*(*e817sd*)/+ heterozygotes are intermediate in phenotype (semi-Dumpy). The phenotype of *dpy-25*(*e817sd*)/*Df* animals was likewise semi-Dumpy, since we could isolate deficiencies covering *dpy-25* by selecting semi-Dumpy progeny of *dpy-25*(*e817*) homozygotes treated with gamma rays. To minimize the possibility of reisolating a single deficiency, we screened only F1 progeny after irradiation. Of approximately 5×10^4 progeny screened, 11 semi-Dumpy progeny were selected; each yielded a strain with both semi-Dumpy and Dumpy animals. Nine of these strains carry deficiencies around *dpy-25*; two strains apparently have second-site suppressors or more complex rearrangements.
16. F. Storfer, thesis, University of Colorado, Boulder, CO (1990). Similar studies have been performed with *Drosophila* [P. Merrill, D. Sweeton, E. Wieschaus, *Development* **104**, 495 (1988)].
17. D. Hall and E. Hedgecock, *Cell* **65**, 837 (1991).
18. R. Waterston, *EMBO J.* **8**, 3429 (1989); R. Barstead and R. Waterston, *J. Cell Biol.* **114**, 715 (1991).
19. D. Miller *et al.*, *Cell* **34**, 477 (1983).
20. Monoclonal antibodies to *unc-54* and *myo-3* products (*19*) are specific to nonpharyngeal muscle. Monoclonal antibodies to paramyosin and vinculin were from Frances and Waterston (*7*), and polyclonal antibody to *unc-22* twitchin was from D. Moerman, G. Benian, R. Barstead, L. Schriefer, and R. Waterston [*Genes Dev.* **2**, 93 (1988)]; these antibodies stain pharyngeal as well as body-wall muscles. The minor and pharyngeal muscles have distinctive positions, not evidently displaced in deficiency homozygotes. Thus, staining in body-wall muscle quadrants by these antisera indicates muscle commitment by the cells normally destined to become body-wall muscles.
21. That the staining outlines four quadrants was confirmed by confocal fluorescence microscopy.
22. Somewhat less severe disorganization was observed in the control deficiency homozygote *ccDf9*. This difference could result either from an effect of *hlh-1* or from effects of flanking genes. Indeed, in a screen of deficiencies in different genetic regions (J. Ahnn and A. Fire, unpublished results), we have observed disorganized muscle in arrested embryos with a variety of severities ranging from complete disorganization of myofilaments to organization indistinguishable from that of wild-type embryos.
23. J. E. Sulston *et al.*, *Dev. Biol.* **100**, 64 (1983).
24. Data not shown.
25. Degenerate (mixed-sequence) primers used were based on highly conserved regions of the basic region and two helices: oligo MWK42 (helix 2 antisense, unbiased), cgagctcRTTNCKNARDATYTCNACYTT; oligo MWK47 (basic region, biased toward *myoD1*), cgaattcAARGCNGCNACNATGMGNGA; oligo MWK127 (basic region, biased toward *myogenin*/*myf6*), tcgaattcGTNAAYSADGCNTTYGA; and oligo MWK136 (helix 1 unbiased), tcgaattcAARGCNGCNACNYTNCGNGA. Sequences in uppercase letters were designed to recognize the myoD gene family (*1, 2*); lowercase letters represent restriction sites added for use in subsequent cloning of the PCR products. R, A or G; Y, C or T; D, A or G or T; K, G or T; S, G or C; and N, A or G or C or T.
26. Adults from a mutant strain that lacked germ cells and wild-type adults had comparable amounts of *hlh-1* mRNA. Thus, the total *hlh-1* mRNA content in the germ line (about 3000 nuclei) is at most a fraction of the total in mature body-wall muscle (95 nuclei).
27. R. Harvey, *Development* **108**, 669 (1990) (*Xenopus*); M. Krause, unpublished results (*Ascaris*).
28. P. Y. Goh and T. Bogaert, *Development* **111**, 667 (1991).
29. To obtain populations of embryos homozygous for each deficiency, we crossed the original strains [*Df*/*dpy-25*(*e817*)] with wild-type males and selected non-dumpy cross progeny. These *Df*/+ animals were then selfed, and the arrested embryos stained and prepared for PCR. If all dead embryos were indeed deficiency homozygotes, then just 25% would be expected to arrest. This was observed for *ccDf1* and *ccDf4*. For *ccDf11*/+, approximately half of the embryos arrested; hence, only about 50% of these arrested embryos were *ccDf11* homozygotes.
30. R Barstead, L. Kleiman, R. Waterston, *Cell Motil. Cytoskeleton* **20**, 69 (1991).
31. H. Epstein, R. Waterston, S. Brenner, *J. Mol. Biol.* **90**, 291 (1974). Note that *unc-54* expression is exclusively zygotic: homozygous *unc-54* null embryos failed to express any *unc-54* myosin even if derived from an *unc-54*(o)/+ mother (*24*).
32. We thank J. Priess for guidance, J. Thomas for help identifiying GLR cells, and C. Mello, A. Shearn, C. Vinson, T. Schedl, S. Tapscott, and S. White-Harrison. Some nematode strains were from the *Caenorhabditis* genetics center, funded by the NIH Center for Research Resources. Supported by NIH grants to A.F. and H.W. M.K. is a W. C. Gibson Fellow of the Muscular Dystrophy Association. A.F. is a Rita Allen Foundation Scholar.

19 November 1991; accepted 24 February 1992

Lithium-Sensitive Production of Inositol Phosphates During Amphibian Embryonic Mesoderm Induction

John A. Maslanski,* LeeAnn Leshko, William B. Busa†

Mesoderm induction and body axis determination in frog (*Xenopus*) embryos are thought to involve growth factor–mediated cell-cell signaling, but the signal transduction pathways are unknown. Li^+, which inhibits the polyphosphoinositide (PI) cycle signal transduction pathway in many cells, also disrupts axis determination and mesoderm induction. Amounts of the PI cycle–derived second messenger, inositol 1,4,5-trisphosphate, increased during mesoderm induction in normal embryos; addition of Li^+ inhibited the embryonic inositol monophosphatase and reversed this increase. Embryonic PI cycle activity thus shows characteristics that indicate it may function in mesoderm induction and axis determination.

Among the earliest developmental decisions made by vertebrate embryos are those that determine the prospective germ layers (endoderm, mesoderm, and ectoderm) and body axes (dorsoventral and anteroposterior). For embryos of the frog, *Xenopus laevis*, experiments involving either cell transplantation or imposition of cell-impermeable filters between blastomeres indicate that mesoderm induction and its corollary, axis determination, begin at about the 32- to 64-cell stage (*1*) and involve secreted diffusible factors that are released from prospective endodermal ("vegetal") cells and act on their overlying equatorial and "animal hemisphere" neighbors (*2, 3*). Three such signals have been proposed to exist (*4*), differing across the prospective dorsoventral axis.

Dorsal and ventral mesoderm-inducing signals may include homologs of the growth factors activin and basic fibroblast growth factor (*3, 5*), but whatever the inducing factors may be, the intracellular signal transduction pathways used in mesoderm induction remain unknown. Involvement of the PI cycle has been suggested on the basis of the teratogenic effect on mesoderm induction of the PI cycle inhibitor Li^+ (*6, 7*). Activation of the PI cycle by calcium-mobilizing hormones or growth factors leads to hydrolysis of the plasma membrane phospholipid, phosphatidylinositol 4,5-bisphosphate, generating inositol 1,4,5-trisphosphate (IP_3), which triggers release of Ca^{2+} from the endoplasmic reticulum into the cytosol, and diacylglycerol, the endogenous activator of protein kinase C (*8*). Lithium inhibits the inositol mono- and bisphosphatases that recycle IP_3 to *myo*-inositol, the precursor of the inositol phospholipids (*9*). Injection of Li^+ into a ventral vegetal cell of the 32-cell *Xenopus* embryo redirects the developmental fates of that cell's progeny toward dorsal mesodermal derivatives and dorsal organizer tissue (*6, 10*). This effect is prevented by co-injection of *myo*-inositol, whereas *epi*-inositol (an isomer not used in the PI cycle) has no effect (*6*). Such isomer-specific rescue implicates the PI cycle as the target of Li^+ and suggests PI cycle involvement in normal mesoderm induction and axis determination. We investigat-

Department of Biology, The Johns Hopkins University, Baltimore, MD 21218.

*Present address: Department of CNS Pharmacology, ICI Americas, Wilmington, DE 19897.
†To whom correspondence should be addressed.

ed Li^+-sensitive inositol phosphate production in *Xenopus* embryos during mesoderm induction.

To test whether teratogenic doses of Li^+ inhibit the embryonic PI cycle, we determined the masses of *myo*-inositol and total inositol phosphates (*11*) with a fluorometric mass assay (*12*). As early as 5 min after Li^+ treatment, embryonic *myo*-inositol mass was depressed and total inositol phosphate mass was increased (Fig. 1), and this effect lasted at least 50 min (approximately two cell cycles). These opposing effects on the substrates and product of inositol monophosphatase are consistent with its inhibition by Li^+ at this teratogenically effective dose and support the "inositol depletion hypothesis" of the teratogenic mechanism of lithium action (*7*).

If PI cycle activity is involved in normal mesoderm induction, then mass changes in IP_3 should coincide with the induction process. Using a commercial IP_3 radioligand-binding assay (*13*) we observed basal IP_3 masses of 74.6 ± 8.0 fmol per embryo at the eight-cell stage (Fig. 2A), equivalent to a concentration of 0.11 μM if distributed homogenously throughout the embryo's cytosolic volume of ~0.65 μl. This value was similar to that determined in preliminary studies of unfertilized eggs and four-cell embryos (*14*). Between the 32- and 64-cell stages, however, total IP_3 mass more than doubled on average, or more than quadrupled when inter-clutch variability was controlled by normalizing data from each clutch. The IP_3 mass remained greater than the basal value through at least the 2048-cell stage. The IP_3 increase reported here is probably due to a specific signaling event rather than, for example, a general upturn in embryonic metabolism because another second messenger, cyclic adenosine 3′,5′-monophosphate (cAMP), did not vary from its basal mass of 1.30 ± 0.28 pmol per embryo by more than 8% between the 16- and 512-cell stages, as determined with radioimmunoassay (embryos from six females).

The elevation of IP_3 mass temporally corresponded with the previously determined onset of mesoderm induction (*1*) and with the period of development during which Li^+ has teratogenic effects (Fig. 2B). Sensitivity to Li^+ was first observed at the 32- to 64-cell stages, slightly preceding or coinciding with the IP_3 increase in normal embryos, and Li^+ sensitivity remained throughout the period over which IP_3 mass was increased. Thus, enhanced PI cycle activity in normal embryos (as evidenced by second messenger accumulation) correlated temporally with both the onset of mesoderm induction and the Li^+-sensitive period of development.

Embryos treated with a teratogenic Li^+ dose at the 128-cell stage showed a significant depression of IP_3 mass from the 512- to at least the 2048-cell stage (Fig. 3). Thus, the burst of IP_3 accumulation accompanying the onset of mesoderm induction was reversed by teratogenically effective Li^+ treatment, in keeping with the hypothesis that PI cycle inhibition is the basis of Li^+-induced teratogenesis (*6*, *7*).

The earliest known step in dorsoventral axis determination is a microtubule-mediated rotation of the zygote's subcortical cytoplasm with respect to the cell cortex that occurs before the first cleavage division. Ultraviolet (UV) irradiation of the zygote prevents this rotation and yields completely ventralized embryos, implicating rotation (some five cell cycles before the first detectable onset of dorsoventral mesoderm induction) in the axis determination process (*15*). We therefore compared IP_3 accumu-

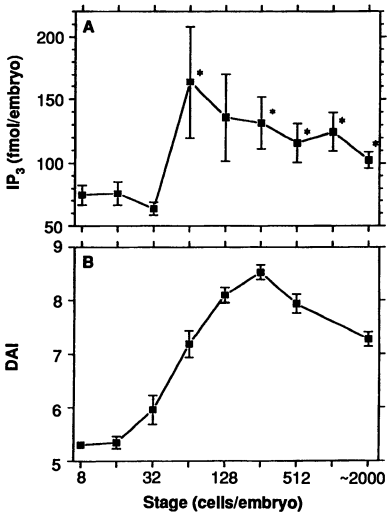

Fig. 2. Time course of (**A**) changes in IP_3 mass in normal embryos and (**B**) sensitivity to Li^+-induced teratogenesis. In (A), embryos were extracted at the indicated stages as described in Fig. 1 and assayed for IP_3 (*13*); embryos from 14 females were used, and each point shown is the mean ± SEM of 12 to 39 determinations (15 embryos per determination). Values marked with an asterisk are significantly greater than the basal (eight-cell) value (one-tailed Student's *t* test, $P < 0.05$). In (B), sibling embryos were treated with 0.3 M LiCl for 6 min at the indicated times and scored for dorsoanterior augmentation on the DAI scale 48 hours later (see Fig. 1).

Fig. 1. Time course of changes in embryonic mass content of (**A**) inositol mono-, bis-, and trisphosphates (IP_{1-3}) and (**B**) *myo*-inositol after a teratogenically effective treatment with LiCl (■) or a treatment with choline chloride (□), which is not a teratogen under these conditions. Embryos from seven females were used. Each symbol is the mean ± SEM of 7 to 16 determinations, except at time = 0 (20 determinations). To reduce inter-clutch variability, we normalized data from the embryos of an individual female to the values at time = 0 for that clutch. Values marked with an asterisk differ significantly from controls (Student's *t* test, $P < 0.05$). Eggs were fertilized in F1 medium and dejellied as described (*6*). At the onset of the 128-cell stage, embryos were transferred to 0.3 M LiCl or choline chloride for 6 min, then washed and returned to F1. At the times indicated, groups of 15 embryos were pooled in a minimal volume of F1 and quick-frozen in dry ice–isopropanol, then extracted and assayed (*12*). Sibling embryos were scored at 48 hours for dorsoanterior augmentation with the dorsoanterior index (DAI), in which a DAI of 5 for a tadpole is normal, a DAI of 10 reflects complete hyperdorsalization, and intermediate scores reflect increasing degrees of dorsoanterior augmentation at the expense of ventroposterior structures (*10*). The DAI scores for Li^+- and choline-treated embryos averaged 9.0 ± 0.1 ($n = 26$) and 5.1 ± 0.1 ($n = 33$), respectively.

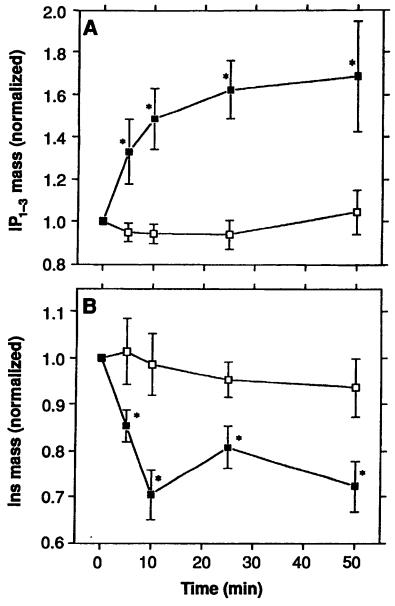

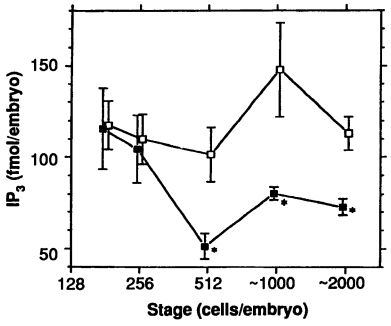

Fig. 3. Time course of reduction of embryonic IP_3 mass by a teratogenically effective Li^+ treatment. Embryos were treated at the onset of the 128-cell stage with 0.3 M LiCl (■) or 0.3 M NaCl (□) and extracted and assayed as described in Fig. 2. Values marked with an asterisk differ significantly from control (NaCl) values (Student's *t* test, $P < 0.05$). The DAI scores for Li^+- and Na^+-treated siblings were 9.0 ± 0.1 ($n = 42$) and 5.1 ± 0.0 ($n = 68$), respectively. Embryos were from four females, and each point is the mean ± SEM of six to ten determinations (15 embryos per determination).

lation in normal embryos to that in embryos that were UV-irradiated as zygotes to block subcortical rotation. The IP_3 mass at the 256-cell stage was not significantly different in UV-irradiated (100.2 ± 10.8 fmol per embryo) and control embryos (103.6 ± 9.0 fmol per embryo) (*16*). Subcortical rotation is therefore not a prerequisite for IP_3 accumulation in the cleavage stage embryo, and our data do not support the suggestion that zygotic UV irradiation should globally enhance PI cycle activity during mesoderm induction (*7*).

Combined with the demonstration of rescue from Li^+-induced teratogenesis by provision of exogenous *myo*-inositol (*6*), our data documenting PI cycle inhibition and depression of IP_3 masses by teratogenic Li^+ treatments strongly support the hypothesis that the effects of lithium on *Xenopus* development depend in large measure on its ability to inhibit the PI cycle signal transduction system. Lithium is also a documented teratogen in human embryos (*17*), in which its mechanism of action remains unknown.

The PI cycle probably functions in normal development, as suggested by both the abrupt rise in IP_3 mass, which is coincident with the onset of mesoderm induction, and the effect of PI cycle inhibition on axis determination. As we shall report (*18*), when mammalian serotonin type 1C receptors (which activate the embryonic PI cycle when stimulated) are expressed dorsally and are activated during mesoderm induction, dorsoanterior specification is blocked in intact embryos, and both convergent extension and transcription of the cardiac actin gene (indicators of mesoderm induction) are inhibited in explants from the animal pole treated with exogenous activin A. Thus, the PI cycle seems to be part of a complex suite of signal transducers involved in induction. One role of the PI cycle, which the data reported here and elsewhere (*6*) suggest, could be as a mediator of the negative feedback signal recently postulated to modulate the induction process (*19*).

REFERENCES AND NOTES

1. E. A. Jones and H. R. Woodland, *Development* **101**, 557 (1987); R. L. Gimlich and J. C. Gerhart, *Dev. Biol.* **104**, 117 (1984).
2. H. Grunz and L. Tacke, *Wilhelm Roux Arch.* **195**, 467 (1986).
3. J. M. W. Slack, B. G. Darlington, J. K. Heath, S. F. Godsave, *Nature* **326**, 197 (1987).
4. L. Dale and J. M. W. Slack, *Development* **100**, 279 (1987).
5. D. Kimelman *et al.*, *Science* **242**, 1053 (1988); T. J. Musci, E. Amaya, M. W. Kirschner, *Proc. Natl. Acad. Sci. U.S.A.* **87**, 8365 (1990); D. Kimelman and M. W. Kirschner, *Cell* **51**, 869 (1987); J. M. W. Slack and H. V. Isaacs, *Development* **105**, 147 (1989); G. Thomsen *et al.*, *Cell* **63**, 485 (1990); M. Asashima *et al.*, *Proc. Natl. Acad. Sci. U.S.A.* **88**, 6511 (1991); R. A. Shiurba *et al.*, *Development* **113**, 487 (1991); L. L. Gillespie *et al.*, *ibid.* **106**, 203 (1989); E. Amaya, T. J. Musci, M. W. Kirschner, *Cell* **66**, 257 (1991); A. J. M. van den Eijnden–Van Raaij *et al.*, *Nature* **345**, 732 (1990); J. C. Smith, B. M. J. Price, K. Van Nimmen, D. Huylebroeck, *ibid.*, p. 729; M. Asashima *et al.*, *Roux's Arch. Dev. Biol.* **198**, 330 (1990); J. M. W. Slack, *Development* **113**, 661 (1991).
6. W. B. Busa and R. L. Gimlich, *Dev. Biol.* **132**, 315 (1989).
7. M. J. Berridge *et al.*, *Cell* **59**, 411 (1989).
8. M. J. Berridge, *Biochem. J.* **220**, 345 (1984); Y. Nishizuka, *Nature* **308**, 693 (1984).
9. L. Hallcher and W. Sherman, *J. Biol. Chem.* **255**, 10896 (1980); M. J. Berridge, C. P. Downes, M. R. Hanley, *Biochem. J.* **206**, 587 (1982); S. R. Nahorski, C. I. Ragan, R. A. J. Challiss, *Trends Pharmacol. Sci.* **12**, 297 (1991).
10. K. R. Kao, Y. Masiu, R. P. Elinson, *Nature* **322**, 371 (1986); K. R. Kao and R. P. Elinson, *Dev. Biol.* **127**, 64 (1988).
11. Two chromatographic fractions (*12*) were assayed: one contained *myo*-inositol and the other contained inositol mono- and higher phosphates. Because the assay is insensitive to inositol tetrakis and higher phosphates under the conditions used here (*12*), the "total inositol phosphates" reported represent only inositol mono- through trisphosphates, of which the mono- and bisphosphates constitute the vast majority.
12. J. A. Maslanski and W. B. Busa, in *Methods in Inositide Research*, R. F. Irvine, Ed. (Raven, New York, 1990), pp. 113–126. Neutralized perchloric acid embryo extracts were separated into distinct inositol phosphate–containing fractions on Sep-Pak Accell Plus QMA cartridges (Waters) by elution with step gradients of triethylammonium hydrogen carbonate (TEAB). Fractions were then vacuum-dried to remove TEAB and were dephosphorylated with alkaline phosphatase. The *myo*-inositol (the product of the dephosphorylation reactions) was quantified by sequential reactions with inositol dehydrogenase and diaphorase; the latter reaction used as substrate the nonfluorescent electron acceptor resazurin (purified by thin-layer chromatography), which was stoichiometrically converted to fluorescent resorufin and quantified at 565- and 585-nm excitation and emission wavelengths on a spectrofluorometer. Calibration curves were determined from internal standards added to some samples just before homogenization of tissues.
13. D-*myo*-inositol 1,4,5-trisphosphate [^3H] assay system (Amersham). Assay reliability was assessed by three means. Potentially interfering compounds in extracts were evaluated by assaying serial dilutions of cell extract supplemented with unlabeled IP_3; results were linear over a tenfold range of dilutions (correlation coefficient = 0.99). Undiluted extracts were supplemented with 0, 0.5, 2, or 5 pmol of unlabeled IP_3, and a plot of picomoles determined versus picomoles added was again linear (correlation coefficient = 0.97). Triplicate determinations of a single extract supplemented with 20 pmol of IP_3 yielded a value of 20.7 ± 1.0 pmol after correction for endogenous IP_3.
14. J. A. Maslanski, unpublished data.
15. J. Gerhart *et al.*, *Development (suppl.)* **107**, 37 (1989).
16. Mean ± SEM (n = 15) for embryos of five females; $P > 0.05$, Student's t test. Zygotes were irradiated in a silica dish above a UV transilluminator (254 nm) for 2 min, beginning 20 min after fertilization. Groups of 30 irradiated or nonirradiated embryos (256-cell stage) were extracted and assayed as described in Fig. 2. Average DAI scores for siblings were 0.8 ± 0.1 (n = 66) for irradiated embryos and 5.2 ± 0.1 (n = 73) for nonirradiated controls.
17. T. H. Shepard, *Catalog of Teratogenic Agents* (Johns Hopkins Univ. Press, Baltimore, MD, ed. 5, 1986), pp. xxi–xxii and 344–346.
18. K. T. Ault, A. Galione, P. L. Harger, W. B. Busa, in preparation.
19. J. Cooke, *Curr. Top. Dev. Biol.* **25**, 45 (1991).

20. Supported by NIH grants HD22879 and HD27546. We thank C. Frasier (Waters Division of Millipore, Incorporated) for generous provision of supplies and equipment.

16 December 1991; accepted 27 February 1992

Diacylglycerol-Stimulated Formation of Actin Nucleation Sites at Plasma Membranes

Aneesa Shariff and Elizabeth J. Luna

Diacylglycerols, which are generated during phospholipase-catalyzed hydrolysis of phospholipids, stimulated actin polymerization in the presence of highly purified plasma membranes from the cellular slime mold *Dictyostelium discoideum*. The increased rate of actin polymerization apparently resulted from de novo formation of actin nucleation sites rather than uncapping of existing filament ends, because the membranes lacked detectable endogenous actin. The increased actin nucleation was mediated by a peripheral membrane component other than protein kinase C, the classical target of diacylglycerol action. These results indicate that diacylglycerols increase actin nucleation at plasma membranes and suggest a mechanism whereby signal transduction pathways may control cytoskeletal assembly.

Changes in cell shape and rapid increases in actin polymerization are early cellular responses to stimulation by chemoattractants or growth factors (*1*, *2*). Although the signaling pathway is unclear, it may include phospholipid metabolism, especially phosphatidylinositide (PI) turnover. One theory is that phosphatidylinositol bisphosphate (PIP_2) in the plasma membrane (PM) directly controls actin assembly through interactions with PI-sensitive actin regulatory proteins, such as profilin and gelsolin (*3*). PIP_2 induces the dissociation of these proteins from actin in vitro potentiating actin assembly. One inconsistency of this mechanism is that in vivo PIP_2 concentrations are at a minimum shortly after chemotactic stimulation when actin polymerization from newly generated free barbed ends is increas-

Cell Biology Group, Worcester Foundation for Experimental Biology, Shrewsbury, MA 01545.